

The Optical Gravitational Lensing Experiment. Optical Monitoring of the Gravitationally Lensed Quasar HE1104–1805 in 1997–2002*

Ł. Wyrzykowski¹, A. Udalski¹, P. L. Schechter²,
O. Szewczyk¹, M. Szymański¹, M. Kubiak¹,
G. Pietrzyński¹, I. Soszyński and K. Żebruń¹

¹Warsaw University Observatory, Al. Ujazdowskie 4, 00-478 Warszawa, Poland
e-mail:

(wyrzykow,udalski,szewczyk,msz,mk,pietrzyn,soszynsk,zebrun)@astrow.edu.pl

² Massachusetts Institute of Technology, 77 Massachusetts Avenue,
Cambridge, MA 02139-4307, USA
e-mail: schech@achernar.mit.edu

ABSTRACT

We present results of the long term monitoring of the gravitationally lensed quasar HE1104–1805. The photometric data were collected between August 1997 and January 2002 as a subproject of the OGLE survey.

We determine the time delay in the light curves of images A and B of HE1104–1805 to be equal to 157 ± 21 days with the variability in the image B light curve leading variability of the image A. The result is in excellent agreement with the earlier determination by Ofek and Maoz.

OGLE photometry of HE1104–1805 is available to the astronomical community from the OGLE Internet archive.

1 Introduction

Time delay between variability pattern in the images of gravitationally lensed quasars has been measured in several cases (*e.g.*, Schechter *et al.* 1997, Kundić *et al.* 1997). Determination of time delay has important consequences, as it makes it possible to measure the Hubble constant at long cosmological distances.

The gravitationally lensed quasar HE1104–1805 with relatively large separation between two images A and B (about $3''$) was discovered by Wisotzki *et al.* (1993). The object has been included to the list of regularly monitored objects by the Optical Gravitational Lensing Experiment (OGLE) at the beginning of the second phase of the project – OGLE-II (Udalski, Kubiak and Szymański 1997) in August 1997. The main goal of this sub-project of the OGLE survey was a determination of the time delay of HE1104–1805.

The quasar was regularly observed up to the end of the 1999/2000 observing season (August 2000) with frequency of one observation per 5–7 days (except for three month period, August–October, each year when the quasar was not visible

*Based on observations obtained with the 1.3 m Warsaw telescope at the Las Campanas Observatory of the Carnegie Institution of Washington.

from the Earth). In this way a unique dataset on the long term photometric behavior of HE1104–1805 was collected. Unfortunately, the main goal of the monitoring – determination of the time delay – has not been accomplished (Schechter *et al.* 2003). It turned out that both images of HE1104–1805 changed the brightness in a rather uncorrelated way making determination of time delay practically impossible.

On the other hand, the large variability of image A of HE1104–1805 on a time scale of weeks was most likely caused by microlensing. Variability of a gravitationally lensed quasar is believed to consist of at least two components: intrinsic variability of the lensed quasar and microlensing variability caused by lensing galaxy. Thus, surprisingly, the dataset collected by OGLE-II provided unique observational material for studying microlensing in gravitational lenses and contributed to better understanding of this phenomenon (Schechter *et al.* 2003).

In November 2000 the OGLE-II phase ended and observations were suspended. After a half year break the OGLE project resumed observations after a significant upgrade of observing capabilities (OGLE-III). HE1104–1805 was still on the list of targets, and the object was regularly observed up to January 2002. Unfortunately, the OGLE-II data pipeline providing photometry of the quasar in the real time was not adjusted to the OGLE-III phase at that time. Therefore, the collected data were stored and photometry of HE1104–1805 from 2001–2002 was not available at the time of our first analysis (Schechter *et al.* 2003).

In the meanwhile Ofek and Maoz (2003) announced a determination of the time delay of HE1104–1805 of 161 ± 7 days. They used the OGLE-II photometry combined with their own observations in the *R*-band collected from 1999 to 2002. The data presented by Ofek and Maoz (2003) indicated that at the time when the OGLE-II suspended observations for the hardware transition to the OGLE-III phase, the B component of HE1104–1805 faded by almost 0.3 mag and the pattern was then followed by the A component providing good opportunity for time delay measurement.

The results of Ofek and Maoz (2003) stimulated us to reduce the data collected during OGLE-III phase (2001–2002) and a few additional observations collected at the end of the OGLE-II phase and not presented in Schechter *et al.* (2003). We also attempted to independently derive the time delay based solely on the OGLE dataset of 1997–2002 which is more uniform (only *V*-band measurements) and accurate than that of Ofek and Maoz (2003). We present our results in this paper.

2 Observations

Observations of HE1104–1805 were made between August 1997 and January 2002 as a subproject of the OGLE-II and OGLE-III surveys. All data were collected with the 1.3-m Warsaw telescope at the Las Campanas Observatory in Chile, operated by the Carnegie Institution of Washington.

Observations collected up to August 2000 were described in Schechter *et al.* (2003). After the conjunction with the Sun the quasar was observed a couple of times in November 2000. Unfortunately, because of autoguider failure at that time in each case five 2 minutes exposures were obtained instead of the standard 10 minute one. The 2 minute images were then aligned, stacked and added before the photometry was derived. Additional observation of HE1104–1805 was obtained in February 2001. This time two standard 10 minute exposures were taken. All these observations were made with the OGLE-II setup described in Schechter *et al.* (2003).

From June 2001 to January 2002, HE1104–1805 was observed with OGLE-III setup, *i.e.*, with the 8192×8192 pixel eight chip mosaic camera (Udalski *et al.* 2002) The frequency of observations was similar as during the OGLE-II coverage. Each observation consisted of two 10 minute exposures and the field was shifted a few arcsec between them.

The new images of HE1104–1805 were reduced in the identical manner as the earlier ones (Schechter *et al.* 2003). Photometry was derived with the DOPHOT photometry program (Schechter, Mateo and Saha 1993). The same comparison stars were used for consistency. The finding chart of HE1104–1805 and positions of comparison stars can be found in Fig. 1 in Schechter *et al.* (2003).

Our Fig. 1 presents the entire light curve of HE1104–1805 collected during OGLE observations. Individual measurements are listed in Table 1 and are also available to the astronomical community in digital form from the OGLE archive:

<http://ogle.astroww.edu.pl>
<ftp://sirius.astroww.edu.pl/ogle/ogle2/HE1104/>

or its US mirror

<http://bulge.princeton.edu/~ogle>
<ftp://bulge.princeton.edu/ogle/ogle2/HE1104/>

3 Time Delay

Looking at the light curves of both images presented in Fig. 1 one can easily see that the light curve of image A is much more variable than that of image B. It has many features that have no counterparts in the light curve of image B. On the other hand, one can also notice a broad 0.3 mag depression in the light curve which occurred near $HJD = 2452000$ and is present in both light curves. This feature occurred first in the light curve of image B and was followed by image A and is the same as that noted by Ofek and Maoz (2003). This strongly suggests variability arising from variability of the lensed quasar. The well defined shape and long duration of this feature should allow determination of time delay.

Unfortunately, as already mentioned, the feature occurred during 2000/2001 season of the quasar visibility period when the OGLE project underwent a major hardware upgrade. Therefore only infrequent observations of HE1104–1805 were possible during that time. As a result there are relatively few points

Table 1
Photometry of HE1104-1805

HJD - 2450000	Q _A		Q _B		CA	
	V	σ_V	V	σ_V	V	σ_V
666.46490	-1.415	0.005	0.283	0.012	-0.388	0.007
666.47390	-1.415	0.005	0.277	0.009	-0.387	0.008
760.84802	-1.357	0.003	0.338	0.007	-0.389	0.006
760.85665	-1.351	0.003	0.327	0.009	-0.385	0.006
762.85473	-1.338	0.004	0.373	0.011	-0.381	0.007
763.85505	-1.354	0.006	0.357	0.010	-0.392	0.007
773.84775	-1.338	0.005	0.362	0.011	-0.393	0.008
773.85593	-1.341	0.005	0.354	0.012	-0.392	0.007
782.84199	-1.372	0.013	0.392	0.016	-0.394	0.013
782.85017	-1.375	0.012	0.365	0.015	-0.393	0.011
783.84383	-1.363	0.015	0.352	0.019	-0.389	0.015
783.85217	-1.375	0.012	0.362	0.014	-0.390	0.012
789.85059	-1.356	0.007	0.361	0.008	-0.385	0.006
792.81232	-1.389	0.006	0.380	0.009	-0.396	0.007
792.82112	-1.395	0.007	0.348	0.015	-0.394	0.009
800.84329	-1.405	0.005	0.385	0.012	-0.403	0.008
800.85268	-1.412	0.012	0.370	0.016	-0.397	0.013
800.86372	-1.388	0.006	0.405	0.018	-0.407	0.010
806.85209	-1.375	0.012	0.380	0.013	-0.390	0.012
806.86044	-1.387	0.013	0.369	0.013	-0.394	0.013
816.86178	-1.386	0.013	0.404	0.016	-0.393	0.014
816.87297	-1.402	0.009	0.381	0.015	-0.388	0.007
817.84615	-1.403	0.018	0.396	0.017	-0.392	0.016
817.85528	-1.395	0.015	0.402	0.014	-0.394	0.013
820.86843	-1.407	0.014	0.393	0.016	-0.402	0.015
833.80560	-1.386	0.012	0.428	0.016	-0.396	0.012
833.81395	-1.368	0.022	0.429	0.024	-0.385	0.021
840.79155	-1.386	0.005	0.402	0.009	-0.390	0.006
840.79989	-1.383	0.008	0.389	0.009	-0.384	0.008
850.81350	-1.324	0.005	0.378	0.008	-0.391	0.005
850.82185	-1.320	0.006	0.376	0.008	-0.385	0.007
864.65372	-1.359	0.004	0.381	0.006	-0.392	0.005
864.66251	-1.366	0.004	0.365	0.008	-0.399	0.005
866.77954	-1.370	0.005	0.370	0.007	-0.392	0.007
866.78846	-1.361	0.004	0.353	0.009	-0.394	0.006
874.76657	-1.351	0.006	0.389	0.009	-0.390	0.007
874.77512	-1.371	0.006	0.376	0.010	-0.391	0.008
878.66866	-1.391	0.004	0.389	0.011	-0.391	0.006
878.67720	-1.390	0.004	0.363	0.010	-0.388	0.007
891.74182	-1.346	0.005	0.430	0.010	-0.386	0.006
891.75040	-1.343	0.006	0.430	0.010	-0.389	0.006
900.64439	-1.312	0.004	0.439	0.008	-0.386	0.005
900.65275	-1.317	0.004	0.433	0.007	-0.390	0.006
909.58239	-1.242	0.005	0.441	0.016	-0.388	0.008
909.59072	-1.262	0.005	0.435	0.015	-0.397	0.008
911.77374	-1.247	0.007	0.459	0.020	-0.376	0.010
911.78210	-1.253	0.007	0.491	0.029	-0.386	0.012
917.68358	-1.227	0.006	0.451	0.019	-0.379	0.009
917.69199	-1.240	0.006	0.461	0.018	-0.387	0.009
921.64575	-1.214	0.004	0.460	0.010	-0.391	0.006
921.65410	-1.228	0.004	0.433	0.011	-0.390	0.008
928.62998	-1.181	0.004	0.459	0.009	-0.382	0.006
928.63834	-1.180	0.005	0.474	0.009	-0.383	0.006
936.57571	-1.157	0.006	0.492	0.013	-0.388	0.007
950.57474	-1.204	0.004	0.464	0.011	-0.381	0.007
950.58309	-1.228	0.006	0.462	0.011	-0.396	0.008
962.52107	-1.243	0.005	0.471	0.009	-0.391	0.006
962.52943	-1.240	0.006	0.476	0.011	-0.387	0.008
966.54958	-1.229	0.016	0.486	0.018	-0.384	0.016

Table 1
Continued

HJD - 2450000	V^{Q_A} σ_V	V^{Q_B} σ_V	V^{CA} σ_V
971.46710	-1.211	0.010	0.496
971.47701	-1.209	0.011	0.502
971.47701	-1.209	0.011	0.502
985.49468	-1.198	0.009	0.479
985.50301	-1.172	0.009	0.491
990.48608	-1.214	0.006	0.491
990.49443	-1.223	0.005	0.493
996.46974	-1.218	0.012	0.484
996.47811	-1.224	0.015	0.501
1011.49065	-1.245	0.005	0.528
1011.49901	-1.238	0.004	0.522
1020.47797	-1.256	0.004	0.528
1020.48633	-1.254	0.004	0.523
1026.47489	-1.265	0.004	0.527
1026.48324	-1.259	0.005	0.563
1036.47650	-1.191	0.006	0.533
1036.46814	-1.198	0.006	0.539
1126.83991	-1.206	0.005	0.480
1126.84826	-1.191	0.005	0.448
1135.83662	-1.242	0.004	0.479
1135.84498	-1.238	0.005	0.465
1143.84217	-1.208	0.010	0.509
1143.85053	-1.211	0.012	0.496
1155.83927	-1.169	0.005	0.477
1155.84763	-1.170	0.004	0.501
1164.81567	-1.203	0.013	0.504
1164.82404	-1.206	0.014	0.493
1174.79099	-1.170	0.006	0.518
1174.79932	-1.172	0.005	0.518
1186.81180	-1.097	0.007	0.519
1186.82014	-1.105	0.008	0.506
1192.75985	-	-	0.523
1192.76819	-1.121	0.008	0.515
1196.78326	-1.096	0.005	0.545
1196.79160	-1.110	0.005	0.530
1203.78371	-1.106	0.007	0.558
1203.79205	-1.112	0.008	0.549
1216.77722	-1.182	0.011	0.540
1216.78557	-1.180	0.012	0.534
1222.76902	-1.158	0.015	0.557
1222.77738	-1.162	0.017	0.541
1224.75571	-1.147	0.008	0.554
1224.76405	-1.171	0.007	0.559
1230.78547	-1.139	0.011	0.482
1230.79383	-1.147	0.010	0.547
1246.70067	-1.165	0.009	0.532
1246.70901	-1.161	0.009	0.528
1254.74656	-1.145	0.016	0.533
1254.75492	-1.141	0.014	0.535
1262.73071	-1.164	0.008	0.500
1262.73907	-1.162	0.007	0.514
1276.59142	-1.070	0.011	0.504
1276.59975	-1.065	0.010	0.513
1281.66500	-1.085	0.008	0.497
1281.67333	-1.061	0.007	0.507
1288.62525	-1.084	0.012	0.492
1288.63359	-1.093	0.009	0.477
1294.62164	-1.110	0.005	0.479
1294.62998	-1.119	0.005	0.474

Table 1
Continued

HJD – 2450000	V^{Q_A} σ_V	V^{Q_B} σ_V	V^{CA} σ_V
1306.60288	-1.133 0.011	0.491 0.015	-0.388 0.013
1306.61120	-1.152 0.011	0.473 0.013	-0.382 0.012
1316.63431	-1.120 0.010	0.490 0.011	-0.388 0.010
1316.64266	-1.135 0.005	0.487 0.010	-0.388 0.007
1321.63638	-1.070 0.006	0.482 0.010	-0.384 0.007
1339.49695	-1.057 0.004	0.501 0.008	-0.387 0.005
1339.50534	-1.056 0.003	0.490 0.009	-0.390 0.004
1345.49811	-1.049 0.006	0.501 0.010	-0.391 0.008
1345.50645	-1.053 0.005	0.511 0.012	-0.387 0.007
1352.45965	-1.053 0.006	0.489 0.013	-0.390 0.009
1352.46797	-1.060 0.006	0.485 0.012	-0.388 0.008
1365.47141	-1.081 0.008	0.497 0.011	-0.383 0.009
1365.47976	-1.084 0.007	0.476 0.011	-0.387 0.007
1373.47231	-1.076 0.004	0.452 0.008	-0.390 0.005
1373.48063	-1.099 0.020	0.470 0.014	-0.387 0.006
1394.48817	-1.065 0.006	0.448 0.010	-0.387 0.007
1394.49649	-1.054 0.005	0.454 0.010	-0.389 0.007
1398.46873	-1.088 0.007	0.499 0.011	-0.396 0.008
1398.47706	-1.083 0.007	0.464 0.010	-0.388 0.007
1489.84879	-1.143 0.008	0.449 0.010	-0.388 0.008
1489.85714	-1.156 0.008	0.452 0.012	-0.388 0.008
1497.85002	-1.100 0.004	0.448 0.011	-0.389 0.006
1512.82977	-1.129 0.005	0.448 0.011	-0.373 0.007
1512.83812	-1.118 0.005	0.464 0.011	-0.382 0.006
1519.82916	-1.133 0.006	0.455 0.009	-0.388 0.013
1519.83753	-1.126 0.009	0.460 0.011	-0.386 0.010
1526.83854	-1.116 0.006	0.435 0.011	-0.392 0.007
1526.84689	-1.109 0.011	0.473 0.013	-0.394 0.011
1542.85348	-1.134 0.010	0.504 0.013	-0.379 0.010
1544.81970	-1.135 0.006	0.517 0.011	-0.388 0.007
1544.82803	-1.138 0.009	0.496 0.011	-0.398 0.010
1552.83863	-1.101 0.010	0.526 0.014	-0.388 0.012
1552.84703	-1.103 0.007	0.514 0.011	-0.389 0.010
1562.84324	-1.065 0.008	0.536 0.013	-0.387 0.008
1562.85157	-1.054 0.007	0.526 0.011	-0.393 0.008
1572.81787	-1.032 0.005	0.516 0.014	-0.392 0.016
1572.82623	-1.030 0.007	0.527 0.014	-0.382 0.009
1581.77920	-1.018 0.008	0.531 0.013	-0.387 0.009
1581.78754	-1.020 0.006	0.507 0.013	-0.377 0.008
1588.77023	-1.010 0.007	0.545 0.012	-0.395 0.013
1588.78201	-1.003 0.007	0.541 0.010	-0.393 0.015
1601.78041	-1.118 0.006	0.538 0.010	-0.387 0.008
1601.78873	-1.115 0.006	0.518 0.010	-0.391 0.007
1608.76978	-1.119 0.005	0.528 0.009	-0.385 0.006
1608.77813	-1.126 0.006	0.535 0.011	-0.385 0.008
1616.75219	-1.129 0.004	0.519 0.008	-0.390 0.006
1616.76053	-1.135 0.003	0.531 0.011	-0.385 0.007
1629.67381	-1.142 0.010	0.533 0.017	-0.386 0.011
1629.68215	-1.160 0.007	0.527 0.012	-0.392 0.009
1634.66890	-1.170 0.007	0.520 0.011	-0.393 0.008
1634.67724	-1.156 0.007	0.541 0.012	-0.389 0.009
1643.64098	-1.096 0.003	0.495 0.009	-0.387 0.005
1643.64934	-1.130 0.005	0.493 0.011	-0.394 0.006
1646.58363	-1.108 0.005	0.506 0.011	-0.385 0.007
1646.59197	-1.110 0.006	0.477 0.015	-0.393 0.007
1659.62581	-1.037 0.004	0.526 0.012	-0.376 0.006
1659.63416	-1.052 0.004	0.511 0.010	-0.388 0.006
1667.59933	-1.049 0.005	0.512 0.010	-0.375 0.007
1667.60776	-1.049 0.006	0.510 0.011	-0.387 0.008

Table 1
Concluded

HJD – 2450000	Q _A		Q _B		CA	
	V	σ_V	V	σ_V	V	σ_V
1675.56667	-1.070	0.004	0.481	0.011	-0.388	0.007
1675.57503	-1.080	0.004	0.501	0.012	-0.389	0.006
1687.53458	-1.088	0.004	0.522	0.009	-0.387	0.005
1687.54291	-1.082	0.003	0.529	0.011	-0.383	0.005
1698.51723	-1.033	0.005	0.538	0.008	-0.383	0.007
1698.52560	-1.035	0.004	0.549	0.008	-0.381	0.006
1705.53958	-1.001	0.004	0.567	0.012	-0.389	0.006
1705.54792	-1.009	0.004	0.548	0.014	-0.392	0.007
1717.46476	-1.000	0.008	0.574	0.011	-0.390	0.008
1717.48314	-1.000	0.014	0.571	0.015	-0.384	0.016
1717.49147	-0.999	0.011	0.592	0.015	-0.374	0.013
1729.48827	-1.018	0.012	0.600	0.014	-0.387	0.012
1729.49661	-1.010	0.011	0.623	0.015	-0.387	0.011
1738.48134	-1.026	0.005	0.610	0.014	-0.400	0.007
1738.48970	-1.018	0.005	0.636	0.015	-0.393	0.008
1748.48952	-1.013	0.004	0.636	0.011	-0.388	0.005
1753.47627	-0.972	0.005	0.645	0.011	-0.391	0.006
1753.48460	-0.969	0.006	0.647	0.011	-0.378	0.008
1759.45499	-1.005	0.011	0.565	0.036	-0.388	0.019
1759.46335	-0.989	0.007	0.658	0.020	-0.393	0.009
1864.81454	-0.986	0.019	0.764	0.052	-0.391	0.011
1864.82704	-0.974	0.009	0.734	0.025	-0.371	0.011
1869.83225	-0.980	0.007	0.786	0.018	-0.387	0.010
1869.84549	-0.981	0.008	0.778	0.020	-0.390	0.011
1874.82956	-0.965	0.008	0.756	0.014	-0.386	0.010
1874.84185	-0.951	0.009	0.746	0.015	-0.387	0.009
1960.62892	-0.694	0.005	0.742	0.010	-0.385	0.006
1960.63726	-0.697	0.005	0.759	0.011	-0.382	0.006
1961.66697	-0.703	0.008	0.750	0.013	-0.385	0.008
1961.67531	-0.698	0.009	0.747	0.011	-0.380	0.009
2072.49533	-0.649	0.005	0.599	0.011	-0.377	0.006
2072.50381	-0.660	0.005	0.585	0.009	-0.381	0.005
2086.47804	-0.699	0.005	0.576	0.010	-0.389	0.005
2086.48652	-0.688	0.004	0.581	0.009	-0.392	0.006
2102.50286	-0.672	0.006	0.572	0.010	-0.392	0.007
2102.51139	-0.675	0.006	0.568	0.010	-0.384	0.007
2123.47288	-0.778	0.008	0.582	0.022	-0.379	0.010
2123.48140	-0.769	0.010	0.584	0.034	-0.376	0.014
2230.85928	-0.871	0.008	0.614	0.021	-0.388	0.010
2233.84468	-0.860	0.008	0.594	0.012	-0.383	0.009
2233.85322	-0.866	0.008	0.613	0.013	-0.387	0.009
2239.84689	-0.831	0.006	0.640	0.013	-0.394	0.007
2239.85545	-0.834	0.007	0.642	0.016	-0.387	0.009
2249.84233	-0.845	0.007	0.631	0.014	-0.386	0.008
2249.85085	-0.837	0.007	0.634	0.014	-0.382	0.009
2253.85220	-0.884	0.005	0.612	0.010	-0.383	0.007
2253.86073	-0.882	0.006	0.616	0.018	-0.391	0.008
2264.83957	-0.871	0.007	0.610	0.010	-0.376	0.008
2264.84811	-0.865	0.006	0.614	0.011	-0.387	0.008
2269.84004	-0.882	0.007	0.624	0.010	-0.386	0.007
2269.84857	-0.883	0.009	0.634	0.012	-0.384	0.009
2269.86228	-0.889	0.009	0.633	0.011	-0.384	0.007
2274.85574	-0.859	0.006	0.633	0.015	-0.383	0.008
2274.86428	-0.863	0.008	0.634	0.015	-0.384	0.008
2280.86288	-0.849	0.006	0.602	0.012	-0.394	0.007
2280.87142	-0.834	0.006	0.636	0.013	-0.392	0.007
2289.86232	-0.795	0.005	0.623	0.010	-0.390	0.006
2289.87087	-0.783	0.006	0.618	0.012	-0.387	0.008
2296.87269	-0.750	0.005	0.619	0.010	-0.383	0.006
2296.88122	-0.741	0.006	0.589	0.013	-0.379	0.008

covering this feature, especially compared to the coverage during the previous observing seasons.

Because the determination of time delay using the entire dataset of images A and B would be dominated mainly by the data taken before the feature occurred such an approach would repeat unsuccessful attempt of Schechter *et al.* (2003). Therefore, we limited our data sample to 51 points, starting at HJD = 2451489.8, *i.e.*, spanning more than a half of the time of all collected data.

To find the time delay between images A and B we used standard χ^2 minimalization. The light curve of image A is steeper than that of image B and image A is also brighter than image B. Therefore we followed Ofek and Maoz (2003) approach and χ^2 fit is described with the following formula:

$$\chi^2 = \sum \frac{(m_{A(t)} - m_{B(t+\tau)} + \alpha(t - t_{\text{mid}}) + \Delta m)^2}{\sigma_{A(t)}^2 + \sigma_{B(t+\tau)}^2} \quad (1)$$

where m_t^A and $\sigma_{A(t)}$ are the magnitude of image A and its error, respectively, as a function of time t ; $m_{t+\tau}^B$ and $\sigma_{B(t+\tau)}$ are the magnitude and error of image B, but at the moment of time shifted by time delay τ ; t_{mid} equals to 2451525.378 and is defined as HJD midpoint between the first and last observations in the dataset analyzed by Ofek and Maoz (2003). It is defined in this manner so that both results could be directly compared. The remaining parameters are the linear trend of image A, α , and magnitude shift between both images, Δm .

Before the fitting procedure was applied all data points were nightly averaged. We decided to make the interpolation of the light curve of image B. The measurements of image B have larger errors because this component is fainter, but, on the other hand, its light curve is much smoother than the light curve of image A.

We applied similar interpolation method as used in Schechter *et al.* (2003): if in data taken within 20 days of the desired time we found two points, we fitted a straight line; if there were three or more we fitted a parabola and in other cases we took a simple average.

The fit was performed for all three parameters τ , α and Δm simultaneously and the global minimum was found at the values of -157 days, 0.064 mag/yr and 1.555 mag, respectively. The minimum had $\chi^2 = 95.6$, what yields $\chi^2/dof = 1.99$, where dof is a number of degrees of freedom and equals here to 48. Fig. 2 shows the χ^2/dof as a function of τ for α and Δm fixed at best fitting values.

Fig. 3 presents the light curve of image A with overplotted light curve of image B, slope corrected and time and magnitude shifted. Only the subset of data that was used for determination of the fit parameters is plotted in Fig. 3.

The upper panel of Fig. 4 presents the composite light curve of both images with the best fit parameters applied for the entire dataset. One can notice that in spite of strong microlensing activity in the light curve of image A the repeatability of smaller long term features in both light curves is rather good what assures that the time delay determination is sound.

The lower panel of Fig. 4 shows the difference between points of the light curve of image A and light curve of image B slope corrected, time and magnitude

shifted and interpolated to the same HJD. Except for clear microlensing scatter in the residuals no long term trend can be noticed. The *rms* of residuals is equal to 0.086 mag.

From χ^2 analysis we estimated the error of the time delay value to be equal to ± 21 days. However, this formal error seems to be somewhat overestimated when we perform the “chi-by-eye” fitting approach. We checked possible time delays by overplotting light curves of both images and concluded that the error should not be larger than ≈ 10 days. Because this result can be somehow subjective we assume further the formal error value of ± 21 days.

4 Discussion

The long term monitoring of HE1104–1805 gravitational lens during the OGLE survey has finally accomplished its original goal. We determined the time delay between the light curve of image A and B to be equal to -157 ± 21 days where the error is the formal error of χ^2 minimalization. In practice it can be somewhat smaller.

Our result is in excellent agreement with that of Ofek and Maoz (2003) who obtained $\tau = -161_{-7-11}^{+7+34}$ days (68% and 95% confidence level). Their result was based on large part of the OGLE dataset (Schechter *et al.* 2003) supplemented with *R*-band observations covering the parts of the light curve crucial for time delay determination (2000–2001 season). One should, however, note that lower accuracy of photometry and necessity of intercalibration of the OGLE *V* and *R*-band data might be a source of additional uncertainty of the Ofek and Maoz (2003) analysis.

The entire OGLE dataset provides now homogeneous *V*-band coverage of the photometric behavior of HE1104–1805 between August 1997 and January 2002. Thus our time delay determination should be less prone for systematic errors.

Additional photometry of HE1104–1805 presented in this paper nicely confirms the features in the light curves noted by Ofek and Maoz (2003). Basically identical time delay from our analysis indicates that the time delay of HE1104–1805 is now determined with good confidence and this gravitational lens increases the still small sample of lenses with well determined time delays. However, one should note slightly different linear trend between the light curves of images A and B. Our value of 0.064 mag/yr is by 0.02 mag larger than that of Ofek and Maoz (2003). It is possible that the discrepancy is caused by less uniform dataset used by Ofek and Maoz (2003) in their analysis.

Acknowledgements. The paper was partly supported by the Polish KBN grants: 2P03D02523 to L. Wyrzykowski and 2P03D02124 to A. Udalski and by a US NSF grant AST-0206010 to P. Schechter. Partial support for the OGLE project was provided by the NSF grants AST-0204908 and NASA grant NAG5-12212 to B. Paczyński.

REFERENCES

- Kundić, T., *et al.* 1997, *Astrophys. J. Letters*, **475**, L85.
- Ofek, E.O., and Maoz, D. 2003, *Astrophys. J.*, **594**, 101.
- Schechter, P.L., Saha, K., and Mateo, M. 1993, *P.A.S.P.*, **105**, 1342.
- Schechter, P.L., *et al.* 1997, *Astrophys. J. Letters*, **475**, L85.
- Schechter, P.L., Udalski, A., Szymański, M., Kubiak, M., Pietrzyński, G., Soszyński, I., Woźniak, P., Żebruń, K., Szewczyk, O., and Wyrzykowski, L. 2003, *Astrophys. J.*, **584**, 657.
- Udalski, A., Kubiak, M., and Szymański, M. 1997, *Acta Astron.*, **47**, 319.
- Udalski, A., Paczyński, B., Żebruń, K., Szymański, M., Kubiak, M., Soszyński, I., Szewczyk, O., Wyrzykowski, L., and Pietrzyński, G. 2002, *Acta Astron.*, **52**, 1.
- Wisotzki, L., Köhler, T., Kayser, R., and Reimers, D. 1993, *Astron. Astrophys.*, **278**, L15.

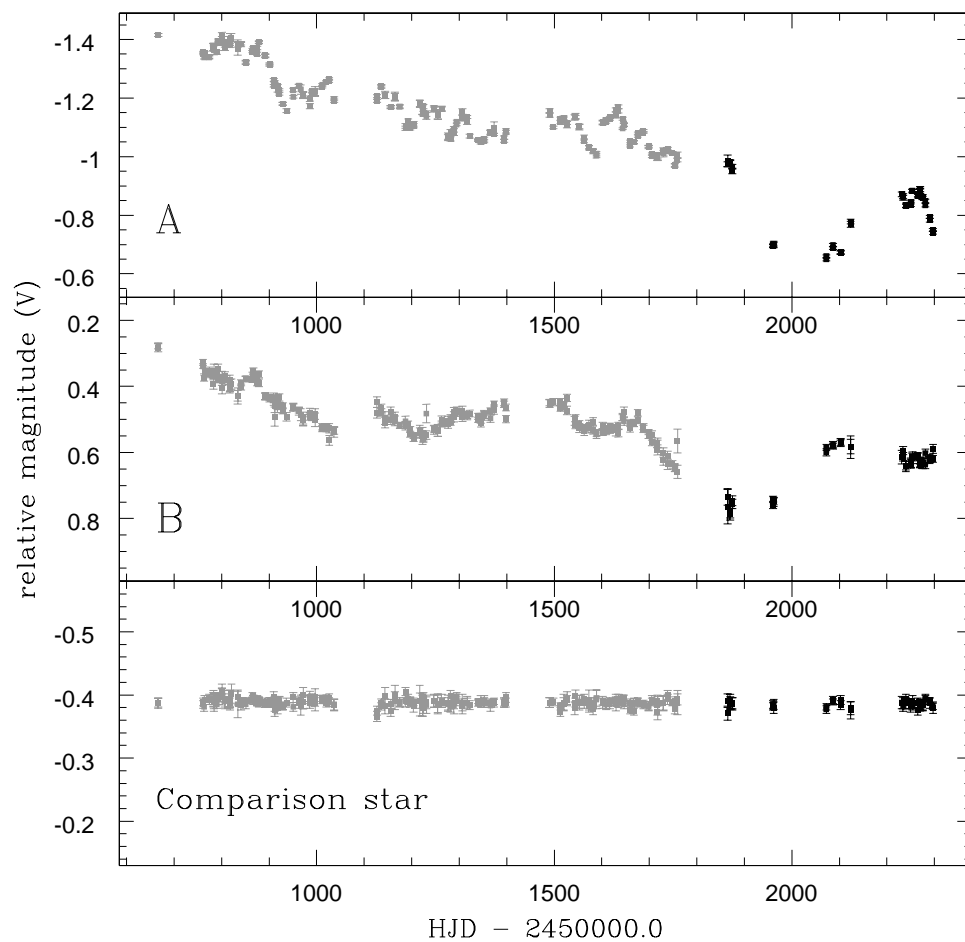


Fig. 1. Light curves of image A (upper panel) and B (middle panel) of the gravitationally lensed quasar HE1104–1805 collected during the OGLE monitoring. In the bottom panel brightness of the nearby comparison stars, CA, is shown. Grey points indicate data presented in Schechter *et al.* (2003).

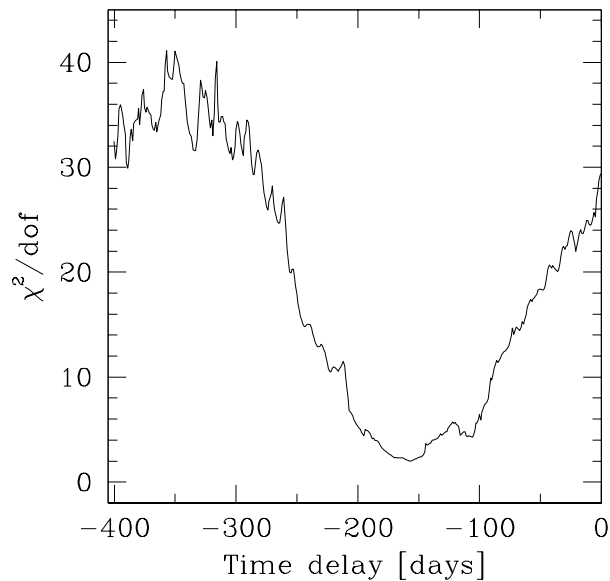


Fig. 2. χ^2/dof as a function of time delay for α and Δm fixed at the best fitting values (0.064 mag/yr and 1.555 mag, respectively). The minimum of $\chi^2/dof = 1.99$ is found for $\tau = -157$ days.

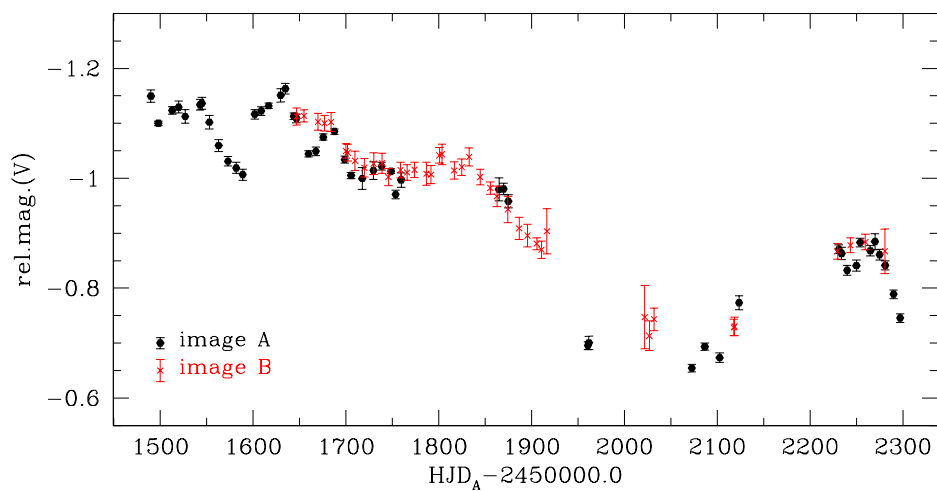


Fig. 3. Superposition of the light curve of image A with the slope corrected ($\alpha = 0.064$ mag/yr), time ($\tau = -157$ days) and magnitude ($\Delta m = 1.555$ mag) shifted light curve of image B. Only data used by the fitting procedure are shown.

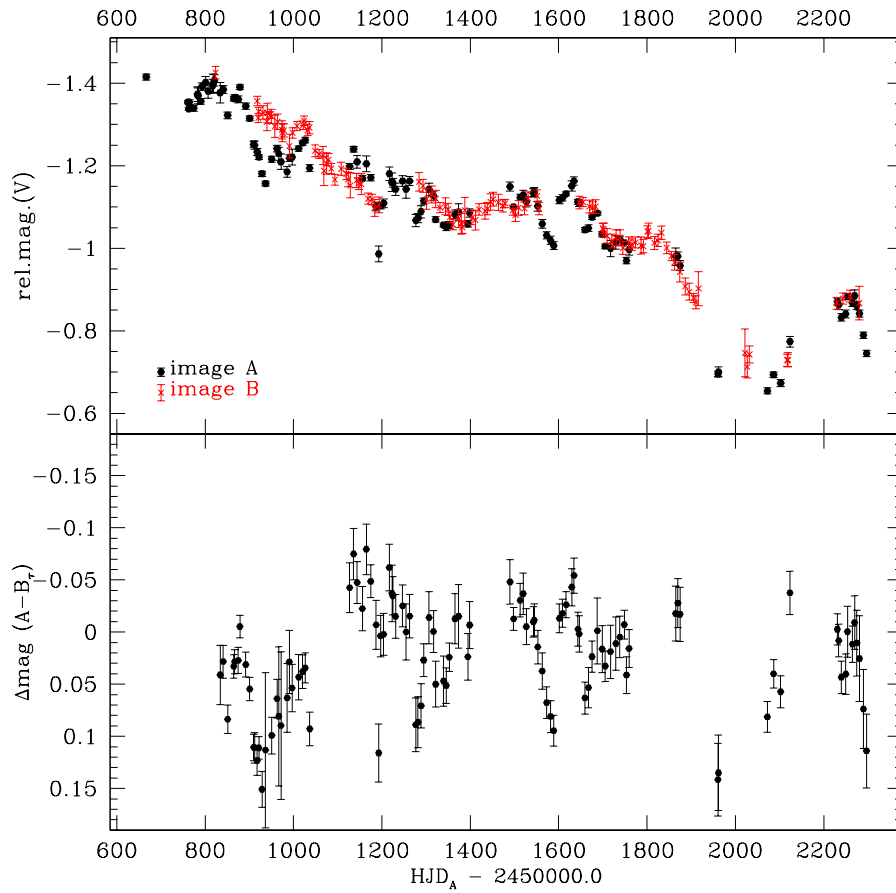


Fig. 4. Upper panel: as in Fig. 3, but with the best fit parameters applied to the entire datasets. Lower panel: the difference between light curve of image A and slope corrected and time and magnitude shifted light curve of image B.